The Effects of Free-Stream Turbulence Intensity on the Aerodynamic Performance of Compressor Cascades

M. Etemadi[1] *- J. J. Defoe*[1] *- R. Taghavi-Zonouz*[2]

[1] Department of Mechanical, Automotive, and Material Engineering, University of Windsor, Windsor, Ontario, Canada, metemadi@uwindsor.ca
[2] Department of Mechanical engineering, Iran University of Science and Technology, Tehran, Iran

ABSTRACT

In this paper we demonstrate non-monotonic behaviour for loss coefficient in a compressor cascade as incident turbulence intensity varies. An experimental investigation of a linear cascade reveals that the interaction of free-stream turbulence with the suction side boundary layer interacts with laminar separation bubbles (LSBs) to set the dominant component of the loss. Turbulence intensity changes were considered as the main parameter to control the size of the LSB. Turbulence grids produced intensities of 1.27%, 2.63% and 4.05% at the blade row inlet. The entropy-based loss coefficient for the suction side boundary layer is determined from the trailing edge momentum thickness and deviation using Denton's correlation. It is found that, up to a critical value, increased turbulence intensity increases the momentum thickness which gives rise to higher overall loss. Further increase in turbulence intensity to values that enable transition before suction surface separation lead to reduced overall losses.

KEYWORDS

compressor cascade, turbulence intensity, laminar separation bubble, boundary layer transition

NOMENCLATURE

C_p Pressure coefficient
d Grid rod diameter
K Roach coefficient
p Pressure
S Pitch
Tu Turbulence intensity
u x-velocity
u_e Boundary layer edge velocity
v y-velocity
x Coordinate along wind tunnel axis
y Coordinate perpendicular to wind tunnel axis in cascade plane
δ Deviation angle
θ Momentum thickness
ξ Loss coefficient

INTRODUCTION

Although flow in gas turbines is generally turbulent, the boundary layer on the compressor blade surfaces are often initially laminar, transitioning to turbulence at some point along the blade chord. In small engines that operate at low Reynolds numbers, laminar flow may persist over the majority of the blade surface. The poor resistance of laminar boundary layers to separation poses a challenge for the design of highly-loaded compressorsin this flow regime. Laminar separations normally result in a transition to turbulent flow with subsequent reattachment of the boundary layer. Quantifying the effects of laminar separation bubbles (LSBs) on compressor blade performance is therefore critical for effective blade design (Stieger, 2003).

Past experimental and numerical work on LSBs provides some initial insight into the mechanisms governing separation-induced transition. Studies carried out on a flat plate with an applied pressure gradient show that vortex roll-up occurs over the separation bubble due to the Kelvin-Helmholtz instability. This is the major mechanism driving transition in separated flows. This finding is well-documented in the literature; see Gaster (1966), Watmuff (1999), McAuliffe and Yaras (2010), Simoni et al. (2012), and Taghavi et al. (2014). Lang et al. (2004) and Marxen et al. (2003) showed that the breakdown of these vortical structures forced transition close to the maximum bubble thickness location. Volino and Hultgren (2001) investigated boundary layer separation, transition, and reattachment by changing the turbulence intensity, Reynolds number, and pressure gradient. They showed that the effects of Reynolds number and turbulence intensity on the behaviour of the boundary layer is not significant unless they are high enough to induce transition in separated flow. In these types of separated flows the separation location and its extent would be highly dependent on the turbulence intensity and Reynolds number. Griffin et al. (2002) showed that increasing free-stream turbulence intensity moves the transition location upstream while, simultaneously, the chordwise length of the transition region is reduced due to a change in the transition mechanism from the natural to the bypass mode. Also, they demonstrated that increasing the Reynolds number will also move the transition point upstream, but found that the length of the transition region is almost independent of the Reynolds number.

While there is a some understanding of the behaviour of LSBs in the literature, aspects related to loss evolution in these types of separated flows is not well understood. In this paper we quantify the effect of LSBs on the performance of a compressor cascade. The effects of free-stream turbulence and Reynolds number on loss are evaluated experimentally. The key finding is that increasing turbulence intensity initially shrinks the LSB but overall losses rise. It is also found that further increasing turbulence intensity moves transition upstream, preventing formation of a LSB and thus decreasing the cascade loss.

APPROACH

The impact of Reynolds number and free-stream turbulence intensity on loss is investigated using a linear cascade at zero incidence. The Reynolds number based on chord varies between 8.0×10^4 and 3.0×10^5 and the incident turbulence intensity is varied from 1.27% to 4.05%.

The blades studied in this paper are Iranian National Gas Turbine Establishment (NGTE) blades with a 10C4/30C50 profile (Felix and Emery, 1957). They are manufactured from acrylic. The first two digits, 10, denote the maximum thickness in percent chord; C4 indicates a thickness distribution, 30 indicates the camber angle in degrees; C refers to the type of camber line, in this case, circular arc; and 50 is the distance of the point of maximum camber from the leading edge in percentage of the blade chord length. Each blade has a chord length of 146 mm (Taghavi and Etemadi, 2013).

The cascade contains three complete blades with half-blades or tailboards on the top and bottom walls as shown in Figure 1. In this way the middle blade performance is representative of an infinite cascade. A comparison of the pressure distributions was performed with an otherwise identical cascade with seven blades (Felix and Emery, 1957) and showed that for the centre blade there was no significant change associated with the reduction in the number of blades. The cascade specifications are summarized in Table 1. More detail on the experimental setup can be found in the work of Taghavi and Etemadi (2013).

Table 1: **Cascade geometry details and operating conditions**

Solidity	1.0
Aspect ratio	1.5
Stagger angle	45°
Incidence angle	0°

Experimental tests are carried out using the open-loop low-speed blower-type wind tunnel at the Aerodynamics Research Center of the Iran University of Science and Technology. The Reynolds number is altered by changing the velocity incident to the cascade. The leading edge of the middle blade of the cascade is located three chords from the wind tunnel exit, where turbulence grids can be installed.

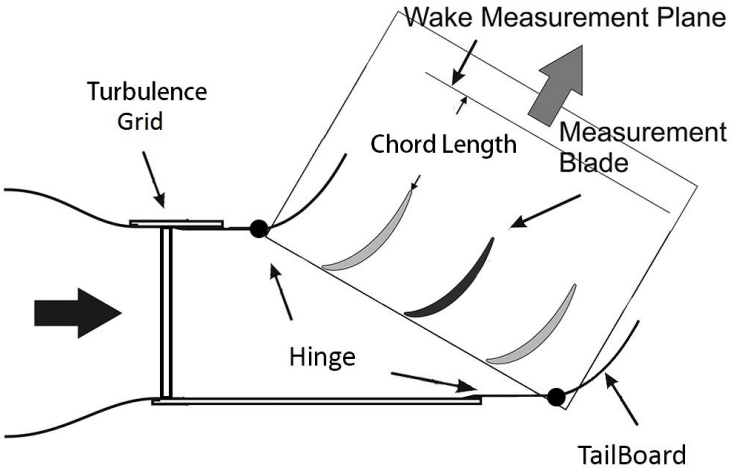

Figure 1: **Schematic view of cascade**

To enable the investigation of a range of turbulence intensities, perpendicular mesh grids (PMGs) are employed. The approach outlined in Roach (1987) provides a design critereon for grid rod size for a desired turbulence intensity at the center blade leading edge. He proposed an empirical correlation for estimating turbulence intensity as a function of the distance downstream of the grid location, x, normalized by the grid rod diameter d. In this approach a constant K is required to calibrate the decay rate of the turbulence intensity. The constant is dependent on the specific experimental setup employed. Roach's empirical equation is:

$$Tu = K(\frac{x}{d})^{-\frac{5}{7}} \tag{1}$$

The coefficient $K = 0.8$ for the experimental setup used in this paper based on a series of hot-wire measurements just upstream of the centre blade. Three turbulence grids were manufactured with target blade leading edge turbulence intensities of 1.25%, 2.5% and 4%.

The turbulence intensities for streamwise and spanwise velocity components are measured, yielding mean values ($\overline{u}$ and $\overline{v}$) and root-mean-squared (RMS) perturbation values (u' and v'). The ratio between u' and v' yields the level of turbulence isotropy. This ratio is measured for all three grids from $x/c = 1.5$ to $x/c = 3.0$. Data at $x/c = 1.5$ is used to assess the isotropy since there is no evidence of a frequency peak in the power spectral density due to the rod wake. At this location it is found that $0.9 \geq u'/v' \geq 1.1$, which indicates that the turbulence is essentially isotropic. The turbulence intensity is calculated as $Tu = u'/\overline{u}$. Although there is a slight change in the turbulence intensity along the pitch due to the 45° stagger angle, it is not thought to be significant since all measurements are performed on the middle blade. The grid dimensions, turbulence intensity, and normalized integral length scale at the leading edge of the centre blade are summarized in Table 2. The integral length scale was estimated by dividing the mean velocity by the integral time scale, which is computed from the autocorrelation of the instantaneous velocities. The turbulence intensities achieved all match the target values to within the uncertainties in the measurements.

Table 2: **Grid details at center blade leading edge**

Grid	x/d	Closed area %	$Tu\%$	Integral length scale/chord
A	338	25	1.27 ± 0.07	0.18
B	130	30	2.63 ± 0.17	0.57
C	70	31	4.05 ± 0.25	1.14

A three-hole probe and a Pitot probe is traversed along the wake measurement plane shown in Figure 1 to capture the outflow angle and total pressure distributions. A 3-axis traversing mechanism, controlled by computer, is used to move the probes with steps of 0.007% chord. The same traversing mechanism is used to measure the inlet total pressure distribution. The measurement locations are defined using Chebyshev's theorem (Clapham, 2009). To obtain the total pressure loss, the mass-averaged total pressures at the inlet and outlet of the cascade are approximated by averaging the data over one pitch, which is possible due to the point distribution used. The same approach is used to determine the outflow angle.

The blade surface pressure distribution is measured at mid-span of the centre blade. Thirty pressure tappings are located at evenly spaced intervals based on arc length. The pressure tappings are connected to piezoelectric gauge pressure transducers through plastic tubes. The pressure sensors are Honeywell 162PC01D with a range from 0 to 1 kPa with accuracy of 0.18% at full scale. A computerised data acquisition system is used to log the surface pressures.

A two cylinder hot-film anemometry probe is used to measure instantaneous fluid velocity, using the same traversing system as for the wake and inlet measurements, enabling detailed boundary layer velocity profiles to be obtained.

Uncertainty quantification is carried out using Jitter analysis as described by Hollman (2001). The uncertainty is determined for all variables at all flow conditions of interest. Representative results are given in Table 3. Small variations in turbulence intensity with Reynolds number were

observed but these are within the measurement uncertainty.

Table 3: **Representative results of uncertainty analysis**

Parameter	Measured Value	Uncertainty
Reynolds Number	160.0×10^3	1.1×10^3
	250.0×10^3	2.0×10^3
	360.0×10^3	3.7×10^3
Turbulence Intensity	1.52% (no grid)	0.08%
	1.27% (grid A)	0.07%
	2.63% (grid B)	0.17%
	4.05% (grid C)	0.25%
Pressure Coefficient	|Max value|=1.5	3.0×10^{-3}
	|Min value|=0.15	1.1×10^{-3}
Total Pressure Loss Coefficient	Max Value = 0.1	2.1×10^{-4}
	Min Value = 0.024	1.2×10^{-4}

RESULTS

Separation, Transition, and Reattachment

The pressure distribution and boundary layer velocity profiles indicate that the separation location is not significantly changed by an increase in turbulence intensity from 1.27% to 2.63%. It can be seen from Figure 2, which depicts the blade surface pressure distribution for an incident turbulence intensity of 4.05%, that at $Re = 160.0 \times 10^3$, the flow does not reattach on the suction surface, as evidenced by the low loading persisting to the trailing edge. The same trend is observed at this Reynolds number for turbulence intensities of 1.27% and 2.63% (not shown). By increasing the Reynolds number to 180.0×10^3, the flow remains fully attached.

The precise separation, transition, and reattachment locations are obtained by analysing the velocity fluctuations. This method is based on the different characteristics of velocity fluctuations in laminar vs. turbulent flow. These fluctuations are shown in Figure 3 for $Re = 100.0 \times 10^3$ and a turbulence intensity of 1.27%. Upstream of the separation bubble, the flow is laminar and the velocity contains only low frequency oscillations (point 1). Transition at low turbulence intensities is due to Kelvin-Helmholtz instabilities wherein turbulent spots are created gradually. These spots create local high frequency perturbations on the mean velocity. The first location at which peaks in the instantaneous velocity are observedis the beginning of the transition process (point 2). Point 3 is located somewhere between the start of transition and the fully turbulent regime. Point 4 is located in the turbulent flow regime, in which oscillations with higher amplitudes are evident. The lack of an underlying sinusoidal variation at point 5 compared to the signal at point 4 indicates that the flow has become re-attached.

The reattachment location is more sensitive to the free stream turbulence intensity: it moves upstream by increasing the turbulence intensity, as indicated in Table 4. The same behaviour is observed when the Reynolds number is changed. This may be related to differing transition mechanisms as freestream turbulence intensity changes. For low values of turbulence intensity,

the inviscid Kelvin-Helmholtz instability is the dominant transition mechanism while for higher turbulence intensity the Klebanoff modes caused by the free-stream turbulence are blended together and contribute simultaneously to the transition process (Hosseinverdi and Fasel, 2015).

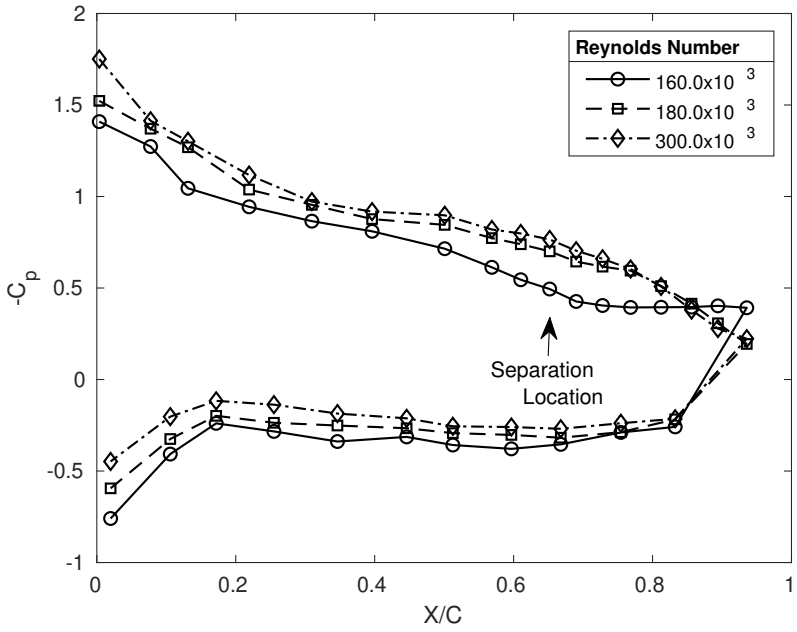

Figure 2: **Pressure coefficient distribution at different Reynolds numbers**

Table 4: **Separation and reattachment locations**

Turbulence intensiy	Reynolds number	Separation location (% Chord)	Transition location (% Chord)	Reattachment location (% Chord)
1.27 %	160.0×10^3	67	95	-
	180.0×10^3	68	90	98
	300.0×10^3	71	88	92
2.63 %	160.0×10^3	69	92	-
	180.0×10^3	70	88	93
	300.0×10^3	72	80	87

Loss Behaviour

Boundary layer parameters are calculated at the trailing edge of the measurement blade using an in-house code to carry out integration on the velocity profile in the boundary layers measured using the hot-film probe. The total pressure loss is computed as described earlier while the suction and pressure side profile loss are computed using Denton's (1993) expression

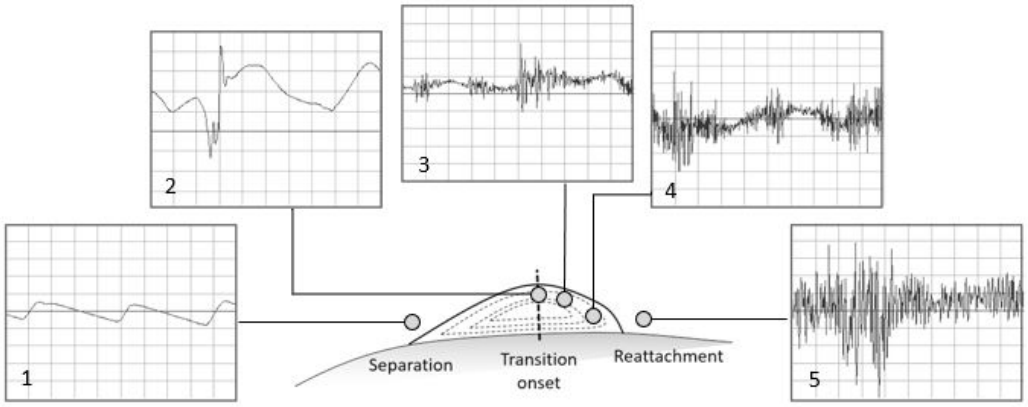

Figure 3: **Fluctuating velocity on the suction surface at $Re = 100,000$ and incoming turbulence intensity of 1.27% (Taghavi and Etemadi, 2014)**

based on momentum thickness and deviation,

$$\xi = \frac{2\theta_{TE}}{Scos\delta} \tag{2}$$

where θ_{TE} is the trailing edge momentum thickness, S is the pitch, and δ is the deviation angle. Loss associated with the endwalls does not affect the flow at midspan, as flow visualization verified that the midspan flow remains well outside the regions affected by secondary flows and endwall boundary layers. Thus the only loss contributions come from the blade surface boundary layers and mixing downstream of the trailing edge. The suction and pressure side profile loss are calculated using Eq. 2 by using velocity profiles and deviation angles at the trailing edge. Mixing loss estimated as the difference between the total pressure loss from one chord downstream and the sum of the suction and pressure side profile loss. The mixing loss is found to always comprise approximately 10% of the total loss, while the suction side loss comprises 50% to 60% of the total.

The total pressure and suction side profile loss coefficients are plotted in Figure 4(a) and 4(b), respectively, vs. Reynolds number. Figure 4(a) shows two distinct characteristics in the loss. First, for all but the lowest Reynolds number considered, increasing turbulence intensity from 1.27% to 2.63% increases loss between 32% and 56% (depending on Reynolds number) while further raising it to 4.05% decreases loss between 20% and 47%. Second, at the lowest Reynolds number considered the loss increases monotonically with Tu because the separation bubble never reattaches to the blade surface (Taghavi et al. (2014)). It can also be seen that this trend is the same for the suction side profile loss in Figure 4(b).

To relate the LSB behaviour discussed earlier to the losses, we combine the results in Table 4 and Figure 4. By increasing turbulence intensity from 1.27% to 2.63%, the LSB size is decreased by 7% and 6% of chord for Reynolds numbers of 160.0×10^3 and 180.0×10^3, respectively. However, the total pressure loss coefficient is increased for each case by 44% and 55%. To determine how a smaller LSB can yield increased loss, we consider the profile

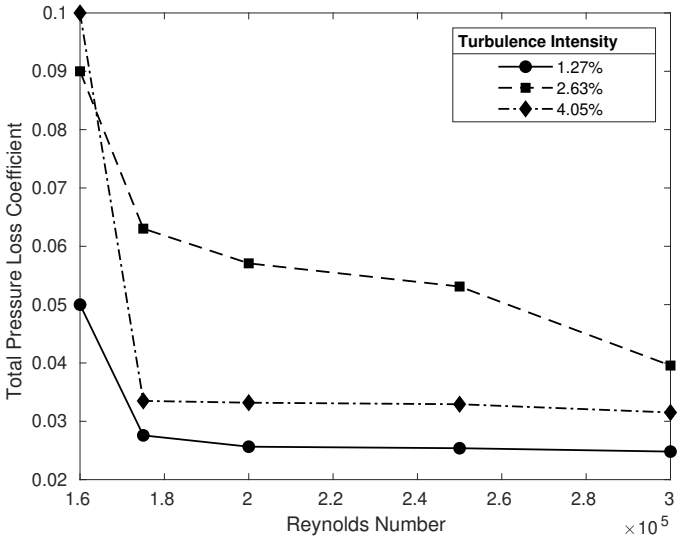

(a)

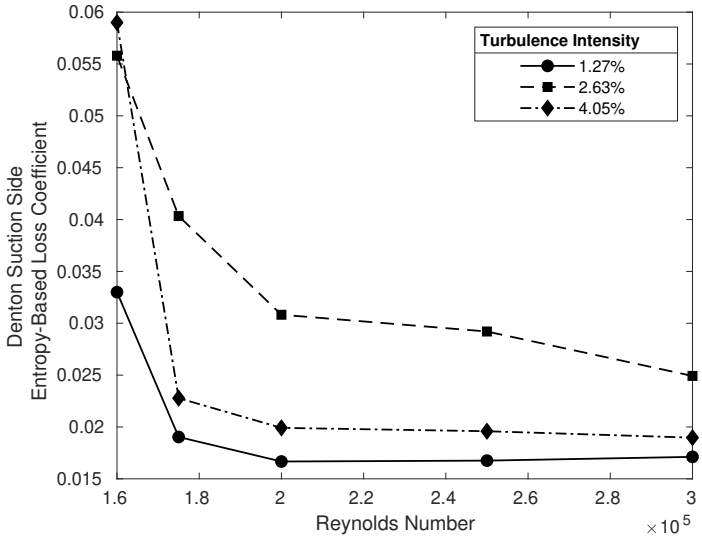

(b)

Figure 4: **Loss variation for different Reynolds number and Turbulence intensities, (a) Total pressure loss coefficient, (b) Suction side profile loss coefficient**

loss. Since the trends for the total loss are matched by the suction side profile loss, we analyze the momentum thickness and the deviation angle to identify the root cause of the increased loss when the LSB size decreases. Figure 5 shows the variations of trailing edge momentum thickness and deviation angle for different turbulence intensities and Reynolds numbers.

Increasing turbulence intensity means that a larger portion of blade experiences attached flow so the cascade can affect increased turning of the flow (Evans 1984). This causes the deviation to decrease by approximatley 0.5° as turbulence intensity increases from 1.27% to 4.05%, meaning the denominator of Eq. 2 increases and the loss would tend to decrease. Thus the increased loss must come from a more than proportional increase in momentum thickness. As

can be seen in Figure 5, the variation of the trailing edge momentum thickness is in agreement with the changes in both suction surface profile loss and overall total pressure loss. Evans (1984) showed that the momentum thickness may either decrease or increase withincreasing fullness of the boundary layer velocity profile depending on whether the added fullness occurs above or below approximately $u/u_e = 0.5$. Combining this with the results shown in Figure 5 means that for profiles very near separation or reattachment most of the effect of increased free-stream Tu occurs in the inner part of the boundary layer (because the velocity near the wall is low) and momentum thickness increases with increasing Tu. For profiles further from separation, the fuller outer profile causes a decrease in momentum thickness.

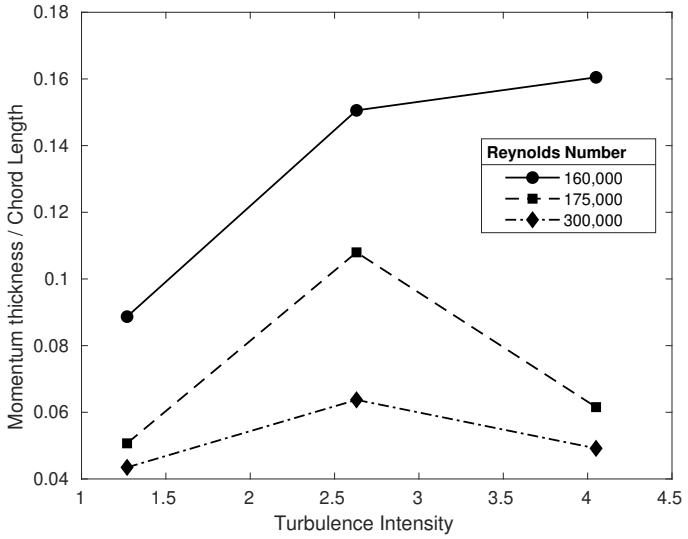

Figure 5: **Momentum thickness variation for different Reynolds numbers and turbulence intensities.**

CONCLUSIONS

The effects of free stream turbulence intensity on midspan loss for a compressor cascade was examined. For all but the lowest Reynolds number considered, the blade experiences a large increase in total pressure loss by increasing the turbulence intensity from 1.27% to 2.63%. By further raising the turbulence intensity to 4.05%, the total pressure loss decreases. At the lowest Reynolds number the loss increases monotonically with increasing Tu because the separation bubble never reattaches to the blade surface. It was shown that the trends for the total pressure loss are mirrored by those of the suction side profile loss. The trailing edge momentum thickness on the suction side and the deviation were explored to find out the root cause of the increase in loss when turbulence intensity was increased from 1.27% to 2.63%, despite the fact that the LSB size is reduced. While deviation is decreased by increasing the turbulence intensity, momentum thickness is increased. Increases in the momentum thickness at higher turbulence intensity are due to the additional momentum entrained into the boundary layer near the wall due to the turbulent eddies. Further increasing the level of turbulence intensity to 4.05% caused the LSB to disappear. The fully attached flow yields reduced loss.

REFERENCES

Clapham, C. and Nicholson J., (2009). Chebyshev's Theorem. In The Concise Oxford Dictionary of Mathematics: Oxford University Press.

Denton, J. D. (1993), The IGTI Scholar Lecture: Loss Mechanisms in Turbomachines. ASME. J. Turbomach. 1993;115(4):621-656. doi:10.1115/1.2929299.

Evans, R.L. (1984). The Effects of Freestream Turbulence on the Profile Boundary layer and Losses in a Compressor Cascade. ASME paper 84-GT-242, 1984

Felix, A. R. and Emery, J. C. A comparison of typical national gas turbine establishment and NACA axialflow compressor blade sections in cascade at low speed. NACA TN 3937, 1957.

Gaster, M. (1966). The structure and behaviour of laminar separation bubbles. In: AGARD CP4 Part 2, pp. 813-854

Griffin P. C., Davies M. D., O′Donnell F. K. , and Walsh E. (2002). The Effect of Reynolds Number, Compressibility and Free Stream Turbulence on Profile Entropy Generation Rate. ASME. Turbo Expo: Power for Land, Sea, and Air, Volume 5: Turbo Expo, Parts A and B ():61-69. doi:10.1115/GT2002-30330.

Hosseinverdi, S. and Fasel, H. (2015). Laminar-turbulent Transition in a Laminar Separation Bubble in the Presence of Free-stream Turbulence. Procedia IUTAM 14: 570-579

Lang, M., Rist, U., and Wagner, S. (2004). Investigations on controlled transition development in a laminar separation bubble by means of LDA and PIV. Exp. Fluids 36, 43-52.

Marxen, O., Lang, M., Rist, U., and Wagner, S. (2003). A combined experimental/numerical study of unsteady phenomena in a laminar separation bubble. Flow Turbulent. Combust. 71, 133-146.

McAuliffe, B., and Yaras, M. (2010). Transition mechanisms in separation bubbles under low and elevated freestream turbulence. ASME J. Turbomachinery. 132, 011004-1-011004-10.

Roach, P.E. (1987). The generation of nearly isotropic turbulence by means of grids. Int. J. of Heat and Fluid Flow 8 (2).

Simoni, D., Ubaldi, M., Zunino, P., and Bertini, F. (2012). Transition mechanisms in laminar separation bubbles with and without incoming wakes and synthetic jet effects. Exp. Fluids 53, 173-186.

Stieger, R., Hollis, D., and Hodson, H., (2003). Unsteady Surface Pressures due to Wake Induced Transition in a Laminar Separation Bubble on a LP Turbine Cascade. ASME Paper No. ASME-GT2003-38303.

Taghavi-Zenouz, R, Etemadi, M., and Nabati, M. (2014). Experimental Investigation of the Loss Coefficients in a Linear Cascade. International Journal of Turbo & Jet-Engines, vol. 31, Issue 2, 149-157.

Taghavi-Zenouz, R. and Etemadi, M. (2013). Newly Developed Empirical Correlations for Simulation of Transitional Flows. Advances in Mechanical Engineering, vol. 5, p. 763197.

Volino, R.J. and Hultgren, L.S. (2000). Measurements in separated and transitional boundary layers under low-pressure turbine airfoil conditions. ASME Paper GT2000-0260.

Watmuff, J.H. (1999). Evolution of a wave packet into vortex loops in a laminar separation bubble. J. Fluid Mech. 397, 119-169.